Two-body densities as a framework for dynamical imaging and their connection to ultra-peripheral collisions

Zaki Panjsheeri, Joshua Bautista, and Simonetta Liuti
University of Virginia Physics Department,
382 McCormick Rd, Charlottesville, Virginia

We present results on two-parton densities in coordinate space which capture a fuller dynamical picture of the proton's internal structure, including information on the relative position between quarks and gluons in the transverse plane. The connection of such two-body densities to observables, proceeds in QCD, via the definition of double generalized parton distributions (DGPDs) that can be accessed in the production of two vector mesons, or two dimuon systems in ultraperipheral collisions (UPCs) through a double scattering process.

DOI: https://doi.org/10.17161/r71z8v22
Keywords: generalized parton distributions, GPD, ultra-peripheral collisions, UPC

1 Introduction

The exclusive process of deeply virtual Compton scattering (DVCS) allows us to access generalized parton distributions (GPDs) [1,2,3] (We refer the reader to Refs.[4,5,6] for reviews on the subject). In turn, GPDs, through Fourier transformation, give spatial information on the charge and matter distributions of the quarks and gluons inside the nucleon [7]. The physical properties derived from the Fourier transforms of GPDs include the spatial distributions of each partonic component of the nucleon in the transverse plane with respect to the proton's motion, as well as the orbital component of angular momentum. Notwithstanding the wealth of information that one could obtain from these Fourier transformed quantities, to capture a fuller dynamical picture of the proton's internal structure, it is fundamental to be able to determine the *relative* position between partons. In order to access information on the relative position of quarks and gluons in a QCD-motivated picture, one needs to define the correlation functions yielding the two-body density distribution in the transverse plane. Connecting the two-body densities to observables, we found that the latter can be defined in QCD through generalized double parton distributions (GDPDs), namely generalized parton distibutions characterized by two hard parton scatterings occurring during the electron-proton or electron-nucleus collision. Using GDPDs, we can define additional observables to describe quark and gluon dynamics, including their overlap probabilities. Such quantities can be extracted from experimental measurements of deeply virtual exclusive processes characterized by multi-particle final states.

2 From one body to two body density

We focus our description on the unpolarized quark inside an unpolarized nucleon described by the GPD, $H^q(X, \zeta = 0, t)$, where x is the quark longitudinal momentum fraction, $t = \Delta^2$ is the four-momentum transfer squared between the initial and final proton, and ζ, the skewness parameter is set to zero. Through Fourier transformation, one obtains the impact parameter-dependent parton distribution function (IPPDF) $\rho(X, \mathbf{b}_T)$, in terms of $\mathbf{b}_T$, the Fourier conjugate to the transverse momentum transfer, $\mathbf{\Delta}_T$ [7,8]. The spatial variables relevant for this problem are described in the left diagram in Figure 1, giving a partonic picture in coordinate space, as first observed using Light Cone (LC) kinematics in Ref.[9].

From the figure, one can see that two relevant variables describe the spatial configuration in a parton-spectator system, namely, $b = b_T$, the relevant transverse distance of the parton from the Center

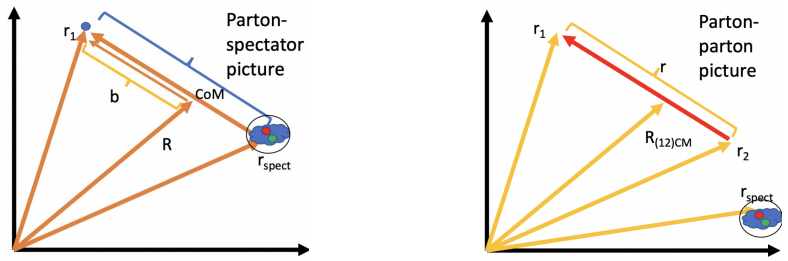

Figure 1 – Spatial coordinates in the transverse plane for one-body distributions (left) and two-body distributions (right).

of Momentum (CoM), and R, the position of the nucleon's CoM. To obtain such a picture through GPDs, we take the correlation function represented in momentum space by Fig. 2,

$$W^{\Gamma}_{\Lambda,\Lambda'} = \int \frac{dz^-_{in}}{(2\pi)} \int \frac{dz^-_{out}}{(2\pi)^2}\, e^{i(k_{in} z_{in})}\, e^{-i(k_{out} z_{out})}\, \langle p', \Lambda' | \overline{\psi}(z_{out})\, \Gamma\, \mathcal{U}(z_{in}, z_{out}) \psi(z_{in}) | p, \Lambda \rangle \Big|_{\substack{z^+_{in(out)}=0 \\ \mathbf{z}_{T,in(out)}=0}} , \quad (1)$$

We represent the four-vectors in LC notation, $v \equiv (v^+, v^-, \mathbf{v}_T)$, $v^{\pm} = (v^o \pm v^3)/\sqrt{2}$, $d^4z = dz^- dz^+ d^2\mathbf{z}_T$;

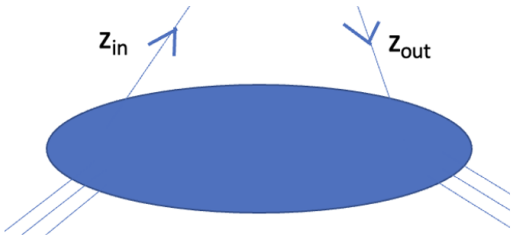

Figure 2 – Correlation function for the GPD in momentum space

we evaluate the fields at equal LC time, $z^+ = 0$. $\psi(z_{in})$, $\bar{\psi}_{out}(z)$ are the quark fields; Γ is an operator between quark fields, *i.e.* either a specific gamma matrix, or a combination of gamma matrices; finally, $\mathcal{U}(z_{in}, z_{out})$, is the link ensuring gauge invariance. In what follows we choose the LC gauge for which $\mathcal{U}(z_{in}, z_{out})$ can be taken equal to one. The field operators product in Eq.(1) is evaluated between an incoming proton state, $|\, p, \Lambda\rangle$, of definite momentum, p, and helicity, Λ, and an outgoing proton state, $|\, p', \Lambda'\rangle$, with momentum, $p' = p - \Delta$, and helicity, Λ'. Taking $\Gamma = \gamma^+$, and Fourier transforming, one obtains [a]

$$\begin{aligned} W^{\gamma^+}_{\Lambda,\Lambda'} &= \int \frac{dz^-}{(2\pi)}\, e^{i(X-\zeta/2)p^+ z^-}\, \langle p' = p - \Delta, \Lambda' | \overline{\psi}\,(0)\, \gamma^+\, \psi\,(z^-)\, | p, \Lambda \rangle, \\ &= \frac{1}{2P^+} \left\{ H_q(X,\zeta,t) \bar{u}(p-\Delta,\Lambda') \gamma^+ u(p,\Lambda) + E_q(X,\zeta,t) \bar{u}(p-\Delta,\Lambda') \frac{\sigma^{i+} \Delta_i}{2M} u(p,\Lambda) \right\}. \quad (2) \end{aligned}$$

Isolating the GPD H for an unpolarized quark inside an unpolarized proton at skewness ζ equal to 0, in momentum space the $H_q(X,0,t)$ is off-diagonal in momentum,

$$H_q(X,0,t) = \int d^2\mathbf{k}_{T,in}\, \phi^*(X, \mathbf{k}_{T,in} - \boldsymbol{\Delta}) \phi(X, \mathbf{k}_{T,in}), \quad (3)$$

and with Fourier transformations of the vertex functions,

$$\phi(X, \mathbf{k}_{in}) = \frac{1}{(2\pi)^2} \int d^2\mathbf{z}_{in}\, e^{i\mathbf{k}_{in}\cdot\mathbf{z}_{in}}\, \tilde{\phi}(X, \mathbf{z}_{in}), \quad (4a)$$

$$\phi^*(X, \mathbf{k}_{out}) = \frac{1}{(2\pi)^2} \int d^2\mathbf{z}_{out}\, e^{-i\mathbf{k}_{out}\cdot\mathbf{z}_{out}}\, \tilde{\phi}^*(X, \mathbf{z}_{out}). \quad (4b)$$

[a] The correlation function's parametrization in terms of GPDs also depends on the QCD evolution scale for the process, and Q^2, that is omitted in these formulae for ease of presentation.

the relationship between the GPD and the IPPDF emerges:

$$H_q(X,0,t) = \int d^2\mathbf{b}\, e^{i\mathbf{b}\cdot\boldsymbol{\Delta}}\, \tilde{\phi}^*(X,\mathbf{b})\, \tilde{\phi}(X,\mathbf{b}) = \int d^2\mathbf{b}\, e^{i\mathbf{b}\cdot\boldsymbol{\Delta}}\, \rho_q(X,\mathbf{b}) \tag{5a}$$

$$\rho_q(X,\mathbf{b}) = \int \frac{d^2\boldsymbol{\Delta}}{(2\pi)^2} e^{-i\mathbf{b}\cdot\boldsymbol{\Delta}} H_q(X,0,t), \tag{5b}$$

where we have defined the transverse space one-body diagonal density distribution. The index q refers to the quark flavor. A similar distribution is ibtained for gluons.

In Figure 3 we show an example of a one-body density distribution, $\rho_g(X,b)$, evaluated for the gluon GPD parametrization from Refs.[10,11], where H_g was constrained by its first moment in X evaluated in lattice QCD [12,13]. Notice that in this case, the gluon distribution depends rather strongly on the scale for the process, Q^2.

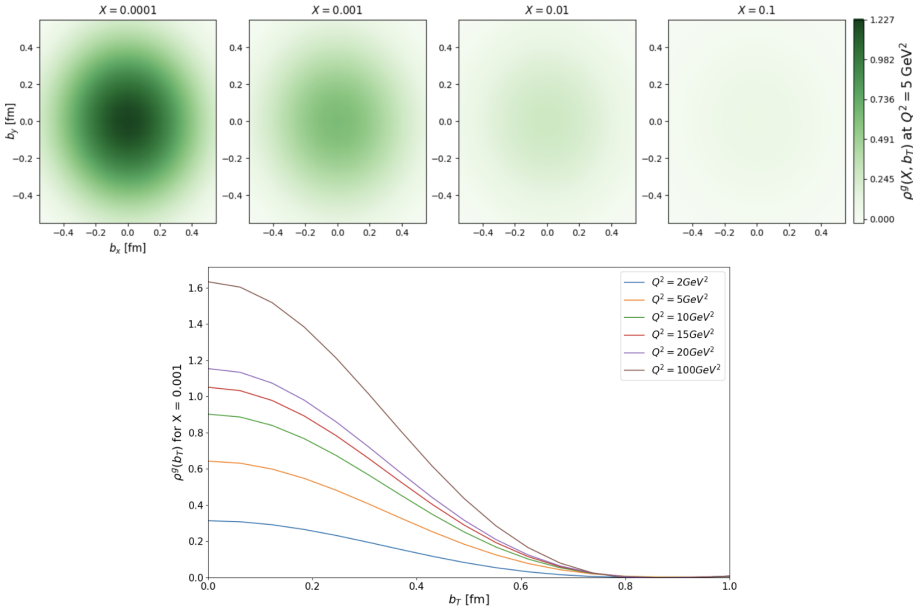

Figure 3 – The Fourier transform $\rho_g(x,b)$ of the unpolarized gluon GPD H_g calculated as a function of x and Q^2.

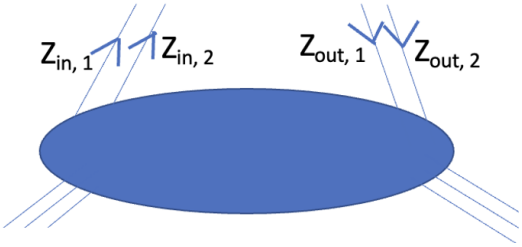

Figure 4 – Two-body correlation function

Although the one-body density distributions already give rich spatial information about the proton's internal structure, as we show in Section 3, in order to study the dynamics of the proton's constituents, we must move from a single-body to a two-body picture, studying now double-parton correlations. We thus introduce the two-body correlation function, as in Figure 4, defined through the following bilinear expression,

$$\begin{aligned} W^{\Gamma}_{\Lambda,\Lambda'} &= \int \frac{dz^-_{1,in} d\mathbf{z}_{1,T,in}}{(2\pi)^3} \frac{dz^-_{2,in} d\mathbf{z}_{2,T,in}}{(2\pi)^3} \int \frac{dz^-_{1,out} d\mathbf{z}_{1,T,out}}{(2\pi)^3} \frac{dz^-_{2out} d\mathbf{z}_{2,T,out}}{(2\pi)^3} \\ &\times e^{i(k_{1,in}z_{1,in}+k_{2,in}z_{2,in})}\, e^{-i(k_{1,out}z_{1,out}+k_{2,out}z_{2,out})} \\ &\times \langle p',\Lambda'|\overline{\psi}(z_{1,out})\,\Gamma\psi(z_{1,in})\,\overline{\psi}(z_{2,out})\,\Gamma\psi(z_{2,in})|p,\Lambda\rangle\Big|_{z_1^+=z_2^+=0} \end{aligned} \tag{6}$$

This definition involving quark fields is similar to the double parton distribution function (DPDF) introduced in [14], but with the initial and final proton states being different, $(p' \neq p)$. Proceeding similarly to

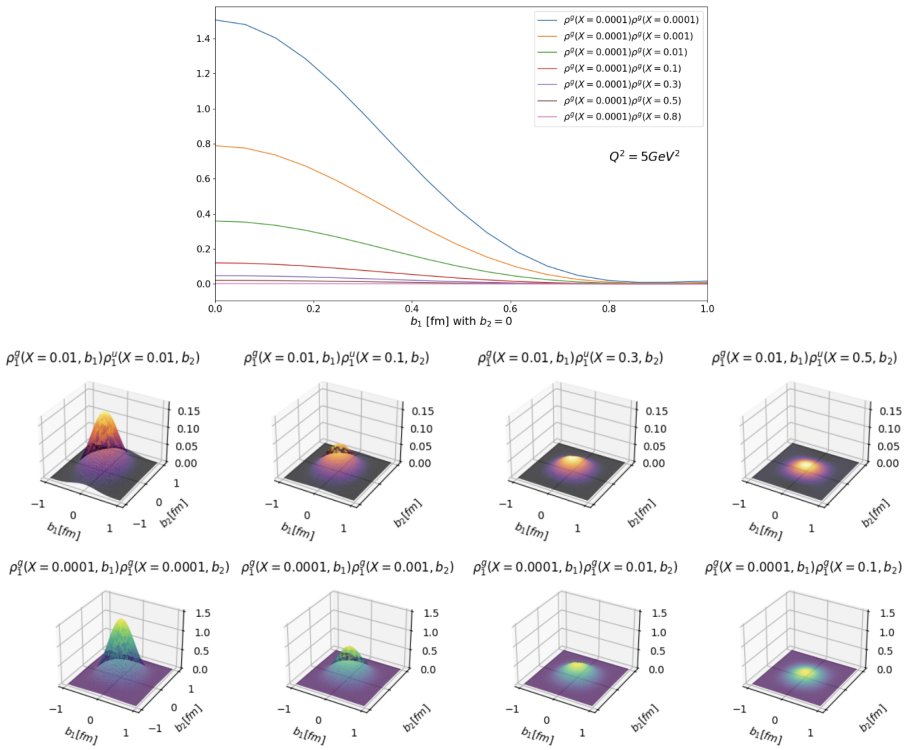

Figure 5 – Visualizing the two-body density as a function of b_1 and b_2 (Eq.9), for different values of x_2, while keeping x_1 fixed.

the one-body case, we can now form the following combinations of the two different quark fields locations, $z_{i,in}$ and $z_{i,out}$, $(i = 1, 2)$, respectively given by,

$$\begin{cases} z_i & = z_{i,in} - z_{i,out} \\ b_i & = \dfrac{1}{2}(z_{i,in} + z_{i,out}) \end{cases} \Rightarrow \begin{cases} z_{i,in} & = b_i + \dfrac{z_i}{2} \\ z_{out} & = b_i - \dfrac{z_i}{2} \end{cases}, \tag{7}$$

as well as the conjugate momenta to b_i and z_i,

$$\begin{cases} \Delta_i & = k_{i,in} - k_{i,out} & \leftrightarrow & b_i \\ k_i & = \dfrac{1}{2}(k_{i,in} + k_{i,out}) & \leftrightarrow & z_i \end{cases} \tag{8}$$

Following a procedure similar to the one-body case, we derived a formulation for the Fourier transform of the four-point correlation function (6), showing that it can be cast in a two-body density form, $\rho_2^{qq}(x_1, \mathbf{b}_1; x_2, \mathbf{b}_2)$, describing the probability of simultaneously finding quark 1 carrying a momentum fraction x_1 at location $\mathbf{b}_1$ and quark 2 carrying a momentum fraction x_2 at location $\mathbf{b}_2$ with respect to the center of momentum of the system. In the absence of correlations in the relative motion of the two quarks, the two-body transverse spatial distribution is described by,

$$\rho_2^{qq}(X_1, \mathbf{b}_1; X_2, \mathbf{b}_2) = \rho_q(X_1, \mathbf{b}_1)\rho_q(X_2, \mathbf{b}_2) \tag{9}$$

where ρ is the diagonal one-body density defined in Eq.(5). Distributions with parton configurations other than qq, *e.g.* qg, or gg, can be written in a similar way, starting from the appropriate two-body correlation function definition.

A visualization of the two-body density distribution, is provided in Fig. 5 where in the upper panel we show a 2D rendition of the gluon-gluon distribution obtained by plotting the quantity, $\rho_2^{gg}(X_1, \mathbf{b}_1; X_2, \mathbf{b}_2)$ at the scale, $Q^2 = 5$ GeV ^{2}, for $X_1 = 10^{-3}$, and fixed $\mathbf{b}_2$, varying X_2 and $\mathbf{b}_1$; in the lower panels, we show 3D versions obtained at $x_1 = 0.01$ (top) and $X_1 = 10^{-3}$, plotted in the $\mathbf{b}_1$, $\mathbf{b}_2$ for various values of X_2.

3 Observables

The average radii described in the previous Section in terms of the Fourier transform of the GPD H for zero skewness are described through the impact parameter dependent PDF (IPPDF), in Figure 6; on the *lhs* we plotted the valence u and we d quark geometric radii compared to the gluon one, at Q^2= 5 GeV^2; on the *rhs* the behavior of the gluon radius with Q^2 is shown. All calculations were performed using the parametrization from Refs.[10,11]. One can see that the gluon radius is much smaller than the quark one, consistent with the geometric representation of baryon junctions, as proposed in Ref.[15] and recently investigated in, *e.g.*, Ref.[16]. Furthermore, we find that, while the radii for all q and g components show a small variation with Q^2 at larger values of $X > 0.01$, at small X, this dependence is substantial, and it should, therefore be more easily detectable in experiment.

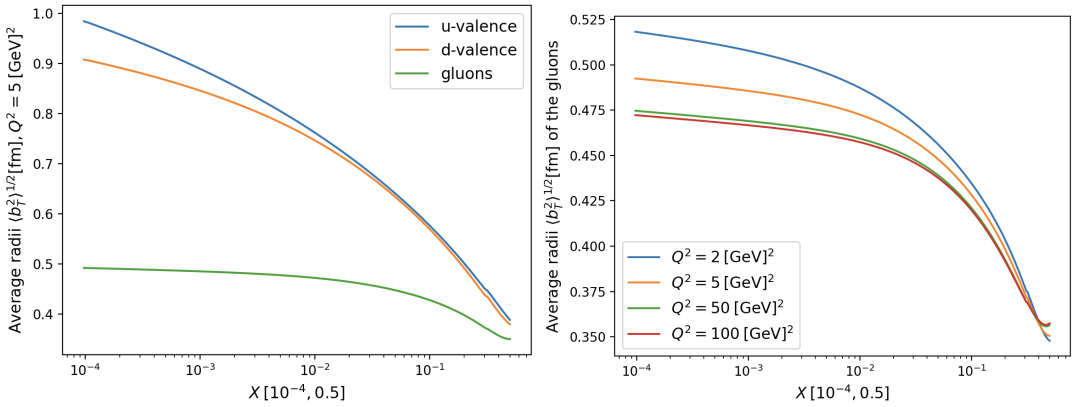

Figure 6 – The average radii for u, d (valence) and g (gluon) distributions (left) provide a quantitative method for extracting spatial information through even the one-body density. We can also study the Q^2-dependence of these average radii through perturbative evolution, as shown for the gluons (right).

From the vectors locating the partons 1 and 2 positions in the transverse plane, $\mathbf{b}_1$ and $\mathbf{b}_2$, respectively, we define the relative distance between them, $\mathbf{r}$, and the distance of the center of mass of the two partons from the origin, $\mathbf{R}_{12}$,

$$\mathbf{r} = \mathbf{b}_1 - \mathbf{b}_2 \tag{10}$$

$$\mathbf{R}_{12} = \frac{\mathbf{b}_1 + \mathbf{b}_2}{2} \tag{11}$$

Defining the root mean squared of their expectation values, one obtains the square average relative distance and average center of mass of the two partons,

$$\langle \mathbf{r}^2 \rangle (X_1, X_2) = \frac{1}{\mathcal{N}} \int\int d^2\mathbf{r}\, d^2\mathbf{R}_{12}\, \left|\mathbf{r}^2\right|\, \rho_2 \left(X_1, \mathbf{R}_{12} + \frac{\mathbf{r}}{2}; X_2, \mathbf{R}_{12} - \frac{\mathbf{r}}{2}\right) \tag{12}$$

$$\langle \mathbf{R}_{12}^2 \rangle (X_1, X_2) = \frac{1}{\mathcal{N}} \int\int d^2\mathbf{r}\, r^2\mathbf{R}_{12}\, \left|\mathbf{R}_{12}^2\right|\, \rho_2 \left(X_1, \mathbf{R}_{12} + \frac{\mathbf{r}}{2}; X_2, \mathbf{R}_{12} - \frac{\mathbf{r}}{2}\right) \tag{13}$$

$$\mathcal{N} = \int\int d^2\mathbf{r}\, r^2\mathbf{R}_{12}\, \rho_2 \left(X_1, \mathbf{R}_{12} + \frac{\mathbf{r}}{2}; X_2, \mathbf{R}_{12} - \frac{\mathbf{r}}{2}\right) \tag{14}$$

The numerical results obtained using our parametrization for the average relative distance, given in Fig. 7, for the specific case of $X_1 = X_2$, correlate with the results for the single parton distributions, in that the distance between a quark of flavor u, d and a gluon field is always larger than the distance of two gluon fields, revealing that gluonic configurations tend to be more compact.

Through the two-body densities we can now address quantitatively the question of whether the u, quarks and gluons will overlap forming localized "hot spots," as suggested in an event-by-event analysis in Refs. [17,18], or whether the gluon field surrounds uniformly the valence quarks.

The geometric average two-parton overlap probability in the transverse plane can be defined as,

$$\langle A(X_1, X_2) \rangle = \frac{1}{\mathcal{N}} \int d^2\mathbf{b}_1 d^2\mathbf{b}_2\, \rho_2^{ij}(X_1, \mathbf{b}_1; X_2, \mathbf{b}_2) A(|\, \mathbf{b}_1 - \mathbf{b}_2\, |),$$

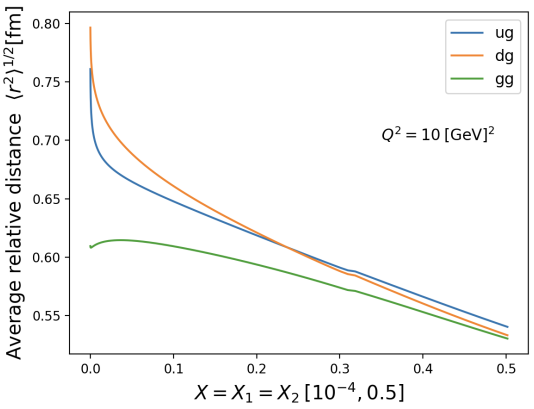

Figure 7 – Average relative distance between the u quark and gluon, the d quark and gluon, and two gluon fields inside the proton plotted vs. $X = X_1 = X_2$, at $Q^2 = 10$ GeV^2.

where $A(r = \mid \mathbf{b}_1 - \mathbf{b}_2 \mid)$ is taken as the geometric area overlap of the two azimuthally symmetric single parton distributions measured in units of an average radius $a = (\langle b_1 \rangle^2 + \langle b_2 \rangle^2)^{1/2}/\sqrt{2}$,

$$A(r) \quad = \quad a^2\pi - \frac{r-\delta}{2}\,(\alpha_1 + \alpha_2) - a_1^2 \arctan\frac{r-\delta}{2\alpha_1} - a_2^2 \arctan\frac{r-\delta}{2\alpha_2} \tag{15}$$

with,

$$\alpha_i = \sqrt{a_i^2 - \frac{(r-\delta)^2}{4}}, \qquad i = 1, 2 \tag{16}$$

and $\delta = a_1 - a_2$.
Performing a change of variables, the average two-parton overlap probability is given as,

$$\langle A(X_1, X_2) \rangle \quad = \quad \frac{1}{\mathcal{N}} \int\int d^2\mathbf{r}\, d^2\mathbf{R}_{12}\, A(r)\, \rho_2^{gg}\left(X_1, \mathbf{R}_{12} + \frac{\mathbf{r}}{2}; X_2, \mathbf{R}_{12} - \frac{\mathbf{r}}{2}\right). \tag{17}$$

Numerical results for the overlap probability are given in Figure 8 for the u quark and gluon case. The figure shows $A(X_1, X_2)$, Eq.(17), plotted vs. X, with $X = X_1 = X_2$, and $Q^2 = 10$ GeV^2, divided by the maximum overlap surface. Putting together results from Figs.6, 7, and 8, we can see that while all parton types tend to be more broadly distributed at low X (Fig.6), thus also spanning broadly distributed relative distances, their overlap probability also increase (Fig.8).

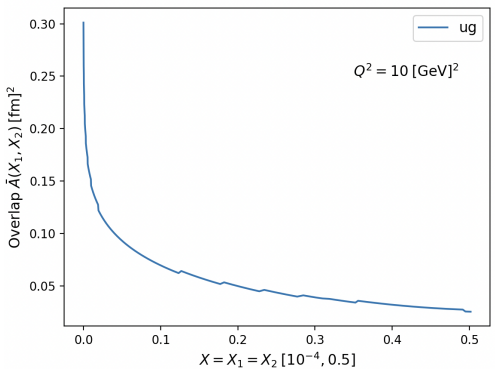

Figure 8 – The overlap probability of the u quark and gluon distributions in the proton plotted vs $X = X_1 = X_2$ for $Q^2 = 10$ GeV^2.

This picture complements the recent BNL approach [19,17,18,20], describing geometrical fluctuations, or event-by-event fluctuations in the proton wave function where the three constituent quarks emit small$-x$ gluons around them, which form "hot-spots" at random locations in the transverse plane.

As first pointed out in Ref.[21] (See also Ref.[22]) in ultraperipheral collisions (UPCs) where, a proton and a nucleus or a proton and a proton collide at impact parameters larger than the sum of the particles'

radii, time-like Compton scattering (TCS), an exclusive process from which one can extract GPDs, may be observed (Fig. 9). We seek to extract GDPDs in double TCS through UPC processes, proposing to use, for example, double vector meson or double dimuon production.

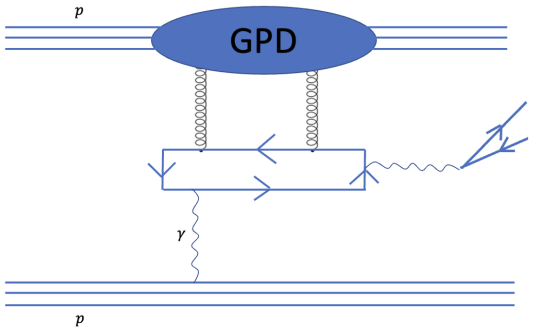

Figure 9 – Connection between UPCs and GPDs

4 Conclusions

We presented results on our study of two-body parton distributions as a means of obtaining information on the relative positions of quarks and gluons inside the proton. While one-body distributions are limited to capturing average static properties of the proton's internal structure, such as the radius covered by various parton distributions, the proton is a complex, multi-body environment, and it is, therefore, more properly imaged through multi-body distributions. As a first step towards the general problem of imaging this multi-body system, and to provide tools to address multiparton correlations beyond the one-body formalism, we studied the geometric correlations between the u and d quark distributions and gluons.

In Refs.[17,18] a connection was provided between the two approaches, "GPDs" on one side, and "geometrical fluctuations" on the other. In particular, the dipole-based description of *coherent* diffractive J/ψ production off a proton was connected to the correlation functions for GPDs, within the collinear framework of QCD. However, the more interesting channel of *incoherent* diffraction, described in terms of double dipole diffraction and leading to small$-x$ gluon fluctuations, or event-by-event, color density geometry driven fluctuations has remained a puzzle in that it could not be rendered, so far, within standard QCD approaches. By introducing two-body correlations functions, we provide a framework to investigate these scenarios and to allow us to study relative spatial configurations of quarks and gluons inside the proton and the atomic nuclei.

Acknowledgments

This research is funded by DOE grant DE-SC0016286.

References

1. Xiang-Dong Ji. Gauge-Invariant Decomposition of Nucleon Spin. *Phys. Rev. Lett.*, 78:610–613, 1997.
2. Xiang-Dong Ji. Deeply virtual Compton scattering. *Phys. Rev.*, D55:7114–7125, 1997.
3. A. V. Radyushkin. Nonforward parton distributions. *Phys. Rev.*, D56:5524–5557, 1997.
4. M. Diehl. Generalized parton distributions with helicity flip. *Eur.Phys.J.*, C19:485–492, 2001.
5. A.V. Belitsky and A.V. Radyushkin. Unraveling hadron structure with generalized parton distributions. *Phys.Rept.*, 418:1–387, 2005.
6. Kresimir Kumericki, Simonetta Liuti, and Herve Moutarde. GPD phenomenology and DVCS fitting - Entering the high-precision era. 2016.
7. Matthias Burkardt. Impact parameter dependent parton distributions and off forward parton distributions for zeta —¿ 0. *Phys. Rev. D*, 62:071503, 2000. [Erratum: Phys.Rev.D 66, 119903 (2002)].
8. M. Diehl. Generalized parton distributions in impact parameter space. *Eur. Phys. J. C*, 25:223–232, 2002. [Erratum: Eur.Phys.J.C 31, 277–278 (2003)].

9. Davison E. Soper. The Parton Model and the Bethe-Salpeter Wave Function. *Phys. Rev.*, D15:1141, 1977.
10. Brandon Kriesten, Philip Velie, Emma Yeats, Fernanda Yepez Lopez, and Simonetta Liuti. Parametrization of quark and gluon generalized parton distributions in a dynamical framework. *Phys. Rev. D*, 105(5):056022, 2022.
11. Gary R. Goldstein, J. OsvaldoGonzalez Hernandez, and Simonetta Liuti. Flexible Parametrization of Generalized Parton Distributions from Deeply Virtual Compton Scattering Observables. *Phys.Rev.*, D84:034007, 2011.
12. P. E. Shanahan and W. Detmold. Gluon gravitational form factors of the nucleon and the pion from lattice QCD. *Phys. Rev. D*, 99(1):014511, 2019.
13. Dimitra A. Pefkou, Daniel C. Hackett, and Phiala E. Shanahan. Gluon gravitational structure of hadrons of different spin. *Phys. Rev. D*, 105(5):054509, 2022.
14. Markus Diehl, Daniel Ostermeier, and Andreas Schafer. Elements of a theory for multiparton interactions in QCD. *JHEP*, 03:089, 2012. [Erratum: JHEP 03, 001 (2016)].
15. D. Kharzeev. Can gluons trace baryon number? *Physics Letters B*, 378(1–4):238–246, June 1996.
16. R. Terra and F. S. Navarra. Charmonium production in high multiplicity *pp* collisions and the structure of the proton. *Phys. Rev. D*, 108:054002, Sep 2023.
17. Heikki Mäntysaari. Review of proton and nuclear shape fluctuations at high energy. *Rept. Prog. Phys.*, 83(8):082201, 2020.
18. Heikki Mäntysaari, Kaushik Roy, Farid Salazar, and Björn Schenke. Gluon imaging using azimuthal correlations in diffractive scattering at the Electron-Ion Collider. *Phys. Rev. D*, 103(9):094026, 2021.
19. Heikki Mäntysaari and Björn Schenke. Accessing the gluonic structure of light nuclei at a future electron-ion collider. *Phys. Rev. C*, 101(1):015203, 2020.
20. Adrian Dumitru, Heikki Mäntysaari, and Risto Paatelainen. Color charge correlations in the proton at NLO: Beyond geometry based intuition. *Phys. Lett. B*, 820:136560, 2021.
21. J. P. Lansberg, L. Szymanowski, and J. Wagner. Lepton-pair production in ultraperipheral collisions at AFTER@LHC. *JHEP*, 09:087, 2015.
22. Ya-Ping Xie and V.P. Gonçalves. Timelike compton scattering in ultraperipheral ppb collisions. *Physics Letters B*, 839:137762, April 2023.